

**Nitrogen and Sulphur Poisoning in Alkene Oligomerization over  
Mesostructured Aluminosilicates (Al-MTS, Al-MCM-41) and  
Nanocrystalline n-HZM-5**

**R. Van Grieken\*, J. M. Escola, J. Moreno and R. Rodríguez**

*Department of Chemical and Environmental Technology, ESCET, Universidad Rey Juan Carlos,  
c/ Tulipan s/n, 28933, Móstoles, Madrid (Spain)*

Published on:

Applied Catalysis A: General 337 (2008) 173–183

[doi:10.1016/j.apcata.2007.12.011](https://doi.org/10.1016/j.apcata.2007.12.011)

\* Corresponding author:

Tel: +34 91 488 70 07

Fax: +34 91 488 70 68

e-mail: [rafael.vangrieken@urjc.es](mailto:rafael.vangrieken@urjc.es)

## Abstract

Oligomerization of 1-hexene in the presence of model poisons such as thiophene (700 – 7000 ppm of sulphur) and n-butylamine (25 – 250 ppm of nitrogen), either alone or in combination, were tested at 200°C, 50 bar and using n-octane as solvent, over three catalysts: two uniformly mesostructured silica-alumina (Al-MTS, Al-MCM-41) and a nanocrystalline HZSM-5 zeolite. A content of 700 ppm of sulphur (adding thiophene) or/and 25 ppm of nitrogen (adding n-butylamine) after a TOS = 240 min. led towards roughly 10 -20% decrease in conversion over nanocrystalline HZSM-5, without significant changes in selectivity. On the contrary, a feeding of 1-hexene with 7000 ppm of sulphur and 250 ppm of nitrogen showed a drastic drop of conversion (from 90 to 27%) over n-ZSM-5 zeolite with a significant increase in the selectivity towards lighter oligomers (dimers, C<sub>7</sub> – C<sub>8</sub> isomers). This fact suggests that the strong acid sites of the zeolite are deactivated by poison adsorption and heavy oligomers/coke deposition both inside the micropores and over the external surface. In contrast, neither Al-MTS nor Al-MCM-41 catalysts were meaningfully affected by the poisons (especially Al-MTS), even for high concentration conditions, due to its high surface area and medium acid strength distribution. TG analyses of the mesoporous catalysts indicate weight losses of ~ 20-25%, with a contribution of 6 to 8% at 400 – 500°C, assigned to the removal of deposited coke. Oligomerization of a FCC effluent under the same conditions over Al-MTS catalyst leads to a remarkable 58% conversion with a oligomer selectivity over 90% (32% of them C<sub>13</sub> – C<sub>18</sub>).

Keywords: poisoning, oligomerization, n-ZSM-5, Al-MTS, 1-hexene

## 1. INTRODUCTION

The oligomerization of light olefins ( $C_2^= - C_7^=$ ) over acid catalysts constitutes a well-established industrial way for the production of hydrocarbon mixtures ( $C_8 - C_{22}$ ), useful as fuels (gasoline, diesel) [1]. The first process dates back to 1934 (Catpoly process) yielding a  $C_6 - C_{10}$  isolefins mixture over the classical Ipatieff catalysts (phosphoric acid supported over Kieselguhr silica clay) [2]. Currently, the most successful oligomerization process is likely the MOGD ("Mobil Olefin towards Gasoline and Distillate") due to its flexibility in terms of the nature of the achieved products. Hence, either gasoline ( $C_5 - C_{12}$ ) or diesel ( $C_{13} - C_{22}$ ) can be attained just by tailoring the operation variables within certain limits ( $T = 200 - 300^\circ\text{C}$ ,  $P = 1 - 5 \text{ MPa}$ ,  $\text{WHSV} = 0.1 - 0.5 \text{ h}^{-1}$ ), using as catalyst a microporous HZSM-5 zeolite [3-7].

Ethylene and propylene, the major building blocks for petrochemicals that come from different processes [8-10], might be used as potential feedstock for acid-catalyzed oligomerization. However, one alternative feedstock may be the light naphta stream stemming from fluid catalytic crackers (FCC). This are mostly made up of  $C_5^= - C_7^=$  alkenes as well as some heavy olefins whose oligomerization towards dimers, trimers, etc. leads to the production of valuable fuels (gasoline, diesel). However, naphta feedstocks coming from FCC contain different sulphur and nitrogen compounds (tiols, thiophene derivatives, amines, etc.) [11] which may poison the oligomerization catalysts. Sulphur concentration in FCC streams vary within 500 – 2000 ppm [12] depending on both the nature of the crackable feedstock (vacuum gasoil, crude residues, etc.) and the operation conditions [13-15]. Both nitrogen and sulphur compounds are amenable to be adsorbed over the acid sites leading towards their deactivation [16]. In addition, they are also believed to be coke precursors [17,18]. In fact, sulphur compounds (e.g.

dimethylsulfide, tetrahydrothiophene, etc.) are known to deactivate HZSM-57 or HZSM-22 zeolites in the oligomerization of light olefins [19].

The most remarkable catalyst used traditionally in the olefin oligomerization is the HZSM-5 zeolite for the MOGD process [20,21]. This is a 10 membered ring zeolite (MFI topology) with two kind of microporous channels (0.51 x 0.55 nm; 0.54 x 0.56 nm) which possesses strong acidity. This zeolite is even capable of yielding near linear isomers when its external surface is deactivated with judiciously chosen blockers (e.g. 2,6,-di-tert-butylpyridine) [22]. Another materials encompassing different porous frameworks and acidities have been also tested in olefin oligomerization, such as zeolites (HZSM-22, Al-TS-1, HZSM-57) [23-25], zeotypes (SAPO-11) [26], amorphous silica-alumina [27] and mesostructured materials (Al-MCM-41, Al-MTS, Al-SBA-15) [28-32]. The catalyst plays a key role as the oligomerization reaction is meant to occur inside the pores [33] and over/close to the external surface [34]. Thereby, the best performances were attained over mesoporous catalysts, mostly Al-MCM-41 and Al-MTS [29,31,35], and small crystal size zeolites (zeolite Beta, nanocrystalline ZSM-5) [34, 35], regardless seemingly of their respective acid strength. Thus, the total selectivity towards oligomers (regarding dimers, trimers and the remaining as a whole) usually exceeds 80% with conversions higher than 70%. The presence of mesopores leads towards longer catalyst lifetimes [28] as the heavy oligomers are better removed from the porous framework [36]. In this regard, the usage of n-paraffin solvents such as n-octane and n-dodecane slows down the deactivation rate increasing the lifetime of zeolite USY and beidellite catalysts [37].

In previous works [31,32,35], both micrometer and nanometer HZSM-5 zeolites and mesoporous aluminosilicates (Al-MCM-41, Al-MTS, Al-SBA-15) were tested in the liquid phase oligomerization of 1-hexene at 200°C and 50 bar using n-octane as solvent. The best

performances in terms of activity and oligomerization selectivity were obtained over hydrothermal Al-MCM-41 and sol-gel Al-MTS due to its mesoporosity ( $D_p \sim 2.0$  nm, BET area  $> 1000$  m<sup>2</sup> g<sup>-1</sup>), as well as nanocrystalline HZSM-5 zeolite, in this case due to the high external surface area (100 m<sup>2</sup> g<sup>-1</sup>). This work is aimed to study in depth the possible application of these catalysts for the oligomerization of a true naphta from FCC units, which contains both nitrogen and sulphur compounds. In order to ascertain both the short and long term potential poisoning effect over the three catalysts, standard mixtures of 1-hexene and the chosen model sulphur (thiophene) and nitrogen (n-butylamine) compound, both alone and in combination, were investigated in the 1-hexene oligomerization under standard conditions ( $T = 200^\circ\text{C}$ ,  $P = 50$  bar). Finally, the best catalyst was tested in the oligomerization of a true naphta coming from a pilot-plant FCC unit.

## 2. EXPERIMENTAL

### 2.1. *Synthesis of the catalysts*

All the catalysts tested in this work were prepared in our laboratory according to procedures previously published elsewhere [38-40]. These catalysts were nanocrystalline HZSM-5 zeolite (n-HZSM-5) [38], hydrothermal Al-MCM-41 [39] and sol-gel Al-MTS [40]. The catalysts were directly synthesized in the acid-protonic form, making unnecessary any ion exchange treatment for providing them acidity.

### 2.2. *Catalyst Characterization*

Powder X-ray diffraction patterns (XRD) were obtained by means of a Phillips X'PERT MPD diffractometer using Cu-K $\alpha$  radiation. XRD patterns within the  $2\theta \sim 0.5 - 10^\circ$  range were

obtained using a step size of  $0.02^\circ$  and a counting time of 10 s. XRD patterns within the  $10 - 80^\circ$  were recorded using a step size and a counting time of  $0.1^\circ$  and 10 s, respectively. The silicon and aluminium content of the catalysts was determined by Inductively Coupled Plasma (ICP-AES) on a VARIAN Vista AX Axial CCD Simultaneous ICP-AES spectrometer. Previously, the sample was digested by acid treatment with  $H_2SO_4$  and HF.

Nitrogen adsorption-desorption isotherms at 77 K were performed in a Micromeritics Tristar 3000 apparatus. The samples were previously outgassed under vacuum at  $210^\circ C$  for 6 hours. The surface area was calculated by means of the BET equation whereas the pore size distributions were determined by the BJH method applied to the adsorption branch of the isotherms. Mean pore size was obtained from the maximum of the BJH pore size distribution. Pore volumes were determined from the nitrogen adsorbed volume at  $P/P_0 = 0.95$ . Micropore volume and external surface area were calculated by application of the t-plot method in a previously selected range of the adsorption branch of the isotherm.

Transmission electron micrographs (TEM) were collected on a Phillips TECNAI 20 microscope equipped with a  $LaB_6$  filament under an accelerating voltage of 200 kV. Prior to the observation, the samples were dispersed in acetone, stirred in an ultrasonic bath and finally deposited over a carbon – coated copper grid.

The acid properties of the catalysts were determined by ammonia temperature programmed desorption (TPD) in a Micromeritics AutoChem 2910 system using He as carrier gas. Previously, the samples were outgassed under a helium flow ( $50\text{ Nml min}^{-1}$ ) with a heating rate of  $15^\circ C\text{ min}^{-1}$  up to  $560^\circ C$  and kept at this temperature for 30 min. After cooling to  $180^\circ C$ , an ammonia flow of  $35\text{ Nml min}^{-1}$  was passed through the sample for 30 min. Once the physisorbed

ammonia was removed by flowing helium at 180°C for 90 min, the chemisorbed ammonia was determined by increasing the temperature with a heating rate of 15°C min<sup>-1</sup> up to 550°C, holding this temperature for 30 min. The ammonia concentration in the effluent helium stream was monitored with a thermal conductivity detector (TCD).

Solid state <sup>27</sup>Al magic angle spinning nuclear magnetic resonance spectra (<sup>27</sup>Al MAS - NMR) were recorded at 104.26 MHz in a Varian Infinity 400 instrument. The sample spinning rate was 11 KHz. 2.5 μs pulses were used and 4000 free induction decays were accumulated with a repetition time of 3 s. These measurements were carried out at room temperature using Al(H<sub>2</sub>O)<sub>6</sub><sup>+3</sup> as external standard reference.

### 2.3. Reagents

The chemicals used in the oligomerization reactions were 1-hexene (98 wt. %), n-heptane (99 wt. %), n-octane (99 wt. %), thiophene (99 wt. %) and n-butylamine (99 wt. %). All of them were purchased from Aldrich. The naphta effluent from pilot-plant FCC unit was provided by REPSOL-YPF. The FCC effluent is mostly made up of a mixture of C<sub>5</sub><sup>-</sup> - C<sub>7</sub><sup>-</sup> olefins and its content in sulphur and nitrogen is the typical of this kind of streams (within the range 600-800 ppm of sulphur and 20-30 ppm of nitrogen).

### 2.4. Experimental setup for the oligomerization reactions

The liquid phase oligomerization reactions were carried out in a Microactivity-Pro Reactor from ICP Engineering and Process Control Group. The equipment consists of a fixed bed tubular reactor of 30 cm length x 0.92 cm internal diameter. In each reaction, the reactor was loaded with

3 g of freshly calcined catalysts. Previously, the catalysts were compressed into wafers, crushed and sieved to use the particle size between 250 and 500  $\mu\text{m}$ . The reactor was heated in a tubular furnace and the temperature was controlled with an axially positioned thermocouple placed inside the catalyst bed.

Initially, the catalysts were activated in the reactor under 50  $\text{Nml}\cdot\text{min}^{-1}$  nitrogen flow at atmospheric pressure for 2 h at 400°C. All the liquid phase oligomerization reactions reported in this work were carried out at 200°C and 5 MPa. The feed consisted of a mixture of 1-hexene (30 wt. %), n-heptane used as internal standard (5 wt %), n-octane as solvent (65 wt %), and the poisons, either alone or in combination: thiophene (700 ppm or 7000 ppm of sulphur) or / and butylamine (25 ppm or 250 ppm of nitrogen). In case of the reactions with the FCC naphtha, this was loaded instead of 1-hexene to the same makeup but neither nitrogen-nor sulphur-containing poisons were added. The reaction mixture was loaded into the reactor with a peristaltic pump using a 0.1  $\text{cm}^3\text{ min}^{-1}$  flow. The weight hourly space velocity (WHSV), referred to 1-hexene basis, was 0.40  $\text{h}^{-1}$  in all the experiments (even in the reaction with the FCC effluent). Steady state was achieved after 180 min of reaction over all the catalysts. After leaving the reactor, the liquid mixture was depressurized to atmospheric pressure and the products collected in a condenser cooled with an ice / water mixture. Gaseous and liquid samples were separated and analysed by gas chromatography (GC) every 60 minutes. On the other hand, catalyst samples were analyzed after reaction to study the nature of the retained products. Mass balances were closed in all the experiments within a  $\pm 8\%$  error.

## 2.5. Analysis of the products

The analysis of the as-obtained liquid and gaseous products was carried out by gas chromatography (GC) in a 3900 Varian GC. The device was equipped with a flame ionization detector (FID) and a 15 m length x 0.25 mm width CP SIL-8CB capillary column. The products were lumped into several fractions based on their respective GC retention times with regards to pure n-paraffins calibration mixtures. Both 1-hexene and its respective isomers (e.g. 2-hexene, 3-hexenes, etc.), which are quickly formed in the reaction, were assigned as “hexenes” in the calculations. In the experiments of 1-hexene oligomerization, the conversion  $X_{\text{hexenes}}$  was defined as  $(\text{mass of converted hexenes}) / (\text{mass of 1-hexene initially loaded}) \cdot 100$ . Selectivity was determined as  $(\text{mass of product fraction}) / (\text{mass of reacted hexenes}) \cdot 100$ . The selectivity calculations were carried out by lumping the products into the following fractions:  $S_{\text{crack}}$  (light C<sub>3</sub>–C<sub>5</sub> hydrocarbons from cracking),  $S_{\text{dimers}}$  (C<sub>9</sub>–C<sub>12</sub> dimers),  $S_{\text{trimers}}$  (C<sub>13</sub>–C<sub>18</sub> trimers),  $S_{\text{heavy}}$  (C<sub>19</sub>–C<sub>30</sub> heavy oligomers) and  $S_{\text{others}}$  (C<sub>7</sub>–C<sub>8</sub> hydrocarbons). In the experiments with the FCC effluent, the conversion ( $X_{\text{effluent}}$ ) was referred to their major components (hexenes, heptenes) as  $(\text{mass of converted hexenes} + \text{heptenes}) / (\text{mass of hexenes} + \text{heptenes initially loaded}) \cdot 100$ . The selectivity calculations were performed regarding identical fractions as before but defined in this case as:  $S_{\text{C3-C5}}$  (light C<sub>3</sub>–C<sub>5</sub> hydrocarbons from cracking),  $S_{\text{C7-C8}}$  (C<sub>7</sub>–C<sub>8</sub> hydrocarbons),  $S_{\text{C9-C12}}$  (C<sub>9</sub>–C<sub>12</sub> hydrocarbons),  $S_{\text{C13-C18}}$  (C<sub>13</sub>–C<sub>18</sub> hydrocarbons),  $S_{\text{C19-C30}}$  (C<sub>19</sub>–C<sub>30</sub> hydrocarbons),.

In addition, the simulated distillation curves according to ASTM D-2887 method of the oligomer hydrocarbon mixtures obtained after 240 min of reaction over the different studied catalysts were determined. Previously, the oligomer mixture was pretreated by microdistillation of a 4 ml reaction volume under identically controlled conditions, in order to remove the volatile compounds (C<sub>3</sub> – C<sub>8</sub> hydrocarbons), mainly unreacted hexenes and the solvent n-octane.

Subsequently, the distillate was dissolved in CS<sub>2</sub> (5 wt%) and analyzed in a 3900 Varian GC equipped with an automatic injector and cryogenic system. The GC was equipped with a flame ionization detector (FID) and on-column injection system inside a 10 m length x 0.53 mm internal diameter capillary column with a 0.17 μm width silicone stationary phase.

### 2.6. Analyses of the catalysts after reaction

The catalyst samples were recovered after reaction and dried under vacuum before being analysed by TG. Thermogravimetric analyses (TGA) of the catalyst samples after reaction were carried out in a TA SDT simultaneous DSC-TGA device under a 50 Nml min<sup>-1</sup> air flow. The heating rate was 5°C min<sup>-1</sup>, starting from ambient temperature up to 600 °C.

## 3. RESULTS AND DISCUSSION

### 3.1. Catalysts characterization.

A thorough discussion about the characterization of the used catalysts has been reported elsewhere [31]. Figure 1a shows the high angle XRD pattern of calcined n-HZSM-5 zeolite while Figure 1b) exhibits the low angle XRD patterns of both mesoporous materials (Al-MCM-41 and Al-MTS). Figure 1a) depicts the XRD pattern of a pure HZSM-5 zeolite, corresponding to a MFI topology without evidence of another crystalline zeolite phase. Additionally, low angle XRD patterns of both Al-MCM-41 and Al-MTS (see Figure 1b)) are typical of these two mesoporous materials. Al-MCM-41 was prepared following a hydrothermal method in basic medium. Consequently, it presents a well resolved XRD pattern with three peaks placed at 3.9, 2.21 and 1.90 nm corresponding to the (1 0 0), (1 1 0) and (2 0 0) hkl planes, respectively. These

reflections are indicative of a rather well formed material. Al-MTS is another uniform mesoporous material but synthesized according to a different procedure, a sol-gel route in acid medium. The XRD pattern of the calcined Al-MTS sample, shown in Figure 1b, only exhibits a main  $d_{100}$  diffraction peak placed at 3.2 nm which is 0.7 nm lower than the observed  $d_{100}$  spacing for the Al-MCM-41 sample. The reflections coming from (1 1 0), (2 0 0) and remaining planes are absent in this case. This fact may be ascribed to the absence of long range order or to the presence of small particle size domains. Therefore, Al-MCM-41 presents a better ordering of their mesopore framework and / or larger particle size domains. These structural differences between both materials (among others) are the origin of the slight differences in catalytic performance observed in other reactions such as catalytic cracking of plastics [41] or 1-octene epoxidation [42].

The main physicochemical properties of the three tested catalysts (n-HZSM-5, HMCM-41 and Al-MTS) are summarized in Table 1. BET surface area of both mesostructured catalysts are around  $1200 \text{ m}^2 \text{ g}^{-1}$  while pore volumes are practically identical ( $0.85 \text{ cm}^3 \text{ g}^{-1}$ ). These values are in close agreement with those previously reported for these samples [39, 40]. The pore size of Al-MTS (1.80 nm) is lower than that of Al-MCM-41 (2.30 nm). Nanocrystalline HZSM-5 presents a BET surface area of  $395 \text{ m}^2 \text{ g}^{-1}$  and an external surface area, determined by the t-plot method, of  $92 \text{ m}^2 \text{ g}^{-1}$ . This means that the share of external / total BET surface area is rather high (about 23.3%) [43]. SEM and TEM micrographs (data not shown) indicates that this sample is made up of 300 – 500 nm aggregates of 20 – 80 nm crystallites [31].

The respective acid properties of the catalysts are summarized in Table 1. All the catalysts were synthesized with practically identical Si/Al atomic ratio (Si/Al = 30). Acidity measurements from ammonia TPD, indicate that n-HZSM-5 shows the strongest acid sites (temperature maximum of ammonia desorption placed at  $355^\circ \text{ C}$ ), as well as the larger acid

character ( $0.32 \text{ meq NH}_3 \text{ g}^{-1}$ ). Both Al-MCM-41 and Al-MTS possess acid sites of medium strength, although those present in Al-MTS seem to be slightly weaker. The coordination state of the aluminium atoms was checked by  $^{27}\text{Al}$  MAS NMR. The three catalysts exhibit a major peak at 55 ppm of tetrahedral aluminium, incorporated into the framework. Only Al-MTS sample shows a contribution of the peak at 0 ppm from octahedral aluminium (extraframework) that accounts for 15 – 20% at most.

### 3.2. Reactions of 1-hexene oligomerization with poisons

The chosen experimental conditions for the oligomerization study were the following:  $T = 200^\circ\text{C}$ ,  $P = 50 \text{ bar}$ ,  $\text{TOS} = 240 \text{ min.}$ , 30 wt.% 1-hexene,  $\text{WHSV} = 0.40 \text{ h}^{-1}$ , in agreement with previous investigations [30,31]. Initially, several experiments were performed with the Al-MTS catalyst in order to check the presence of external mass transfer limitations. Thereby, three flow rates ( $0.1$ ,  $0.08$  and  $0.06 \text{ cm}^3 \text{ min}^{-1}$ ) were tested with different amount of catalysts (3, 2.4 and 1.8 g, respectively), the WHSV being almost the same. The conversion values for the two first experiments were rather similar (76 and 81%) while for the third, it dropped to 57%. Additionally, the selectivity results (data not shown) only changed meaningfully for a flow rate of  $0.06 \text{ cm}^3 \text{ g}^{-1}$  and 1.8 g of catalyst. Therefore, 3 g of catalyst and  $0.1 \text{ cm}^3 \text{ g}^{-1}$  were selected for all the subsequent oligomerization study as it was concluded the absence of external mass transfer constraints in these conditions.

The reactions occurring in the 1-hexene oligomerization are described in the scheme shown in Figure 2. Initially, the 1-hexene is quickly isomerized to a mixture of different hexenes mostly, 2-hexene, 3-hexene by double bond shift due to the low activation energy of this reaction (path 1). The hexene mixture may undergo true oligomerization (path 2) giving rise to the

formation of dimers ( $C_{12}^{\equiv}$ ), trimers ( $C_{24}^{\equiv}$ ), etc. Additionally, both the hexene isomers and the oligomers may be cracked (paths 3 and 4) bringing about a mixture of hydrocarbons which are oligomerized to yield the final  $C_8 - C_{35}$  mixture (path 5). These reactions are also accompanied by skeletal isomerization and hydrogen transfer reactions. The latter are responsible for the appearance of saturates (alkanes), polyenes and different aromatics.

The presence of poisons may affect this whole scheme of reactions as they are all acid – catalyzed reactions modifying both activity and selectivity. Two model poisons were chosen: thiophene and n-butylamine as compounds representative of the sulphur and nitrogen compounds typically found in FCC effluent streams. In fact, thiophenes and its derivatives (alkylthiophenes) account for 60% of the total sulphur compounds present in gasolines [17]. Initially, the experiments were performed loading each poison individually and subsequently, they were mixed up to ascertain their combined effect.

Table 2 summarized the results obtained in the oligomerization of the 1-hexene mixture containing 700 ppm of sulphur in the feed. This is a typical concentration found in FCC effluents (600 – 800 ppm). Conversion values for mesostructured materials remains practically identical, within 75 – 80% range regardless of the presence of the poison thiophene. Likewise, the selectivity towards the different product fractions (dimers, trimers, heavy, etc) over Al-MTS was very similar to those reported without poisons [31]. Hence, the selectivity towards dimers, trimers and heavy oligomers was around 30 - 33% with or without the poison. Consequently, the presence of thiophene does not impair the Al-MTS performance, at least after a TOS = 240 min. In the case of Al-MCM-41 catalyst, only a slight modification in selectivity towards heavier oligomers products may be envisaged. Thereby, the selectivity towards dimers diminishes from 37.6 to 31.5 accompanied with a parallel enhancement of the selectivity to heavy hydrocarbons

(from 26.9 to 31.5). Additionally, cracking selectivity rises up to 5% while it is just 2% without the poison. For the case of n-HZSM-5 catalyst, the changes are more clear than those obtained with the two mesostructured materials. Thus, a 10% drop in conversion may be observed in the oligomerization of 1-hexene with thiophene present in the feed when n-HZSM-5 is used as catalyst. Additionally, the selectivity towards dimers rises while that of trimers diminishes slightly. This is indicative of a slight trend towards lighter oligomers over this catalyst when poison thiophene is added.

In a next step, the poisoning effect of the nitrogen compounds was ascertained by adding n-butylamine (25 ppm of nitrogen) to the 1-hexene feed (e.g. it is known that amines neutralizes strong acid sites in the hydroisomerization of n-decane [18]). No thiophene was included in the reacting makeup. The results obtained in the oligomerization of 1-hexene + 25 ppm of nitrogen as n-butylamine under the standard reaction conditions ( $T=200^{\circ}\text{C}$ ;  $P = 50 \text{ bar}$ ;  $\text{TOS} = 240 \text{ min}$ ) are summarized in Table 3. It should be borne in mind that these results correspond to a TOS = 240 min after reaching steady state operation. The conversion attained over Al-MCM-41 is close to that without poison ( ~80%) while for Al-MTS decreases just slightly. In contrast, over n-HZSM-5 catalyst a sudden drop of conversion is appreciated since it decreases roughly a 15%. Again, the activity of this catalyst is impinged by the presence of the poison n-butylamine in the feed. The selectivity results differ solely, with regards to those without poisons, in a slight increase in the yield of light hydrocarbons, either from cracking ( $\text{C}_3 - \text{C}_5$ ) or others ( $\text{C}_8 - \text{C}_9$  indeed) over the three catalysts. This is especially true over Al-MTS where the sum  $S_{\text{crack}} + S_{\text{others}}$  add up to almost 9%, being accompanied by a parallel decrease of the trimers selectivity. In contrast, over Al-MCM-41 a weak trend towards trimers is appreciated. On the other hand, the oligomerization selectivity results over n-HZSM-5 are rather similar to those obtained in the absence of poisons.

However, the real situation is to find both poisons in the feed to the oligomerization unit. To ascertain the combined effect of both poisons, model mixtures formed by 1-hexene + 700 ppm of sulphur + 25 ppm of nitrogen were tested. In addition, a highly concentrated mixture of 1-hexene + 7000 ppm of sulphur + 250 ppm of nitrogen was also investigated. The purpose of the latter tries to represent the long term performance of the catalysts, increasing the level of poisoning to speed up the changes induced in these conditions. Figure 3 illustrates the results with both model mixtures compared with the non poisoned feed. In terms of activity, the usage of a mixture made up of 700 ppm sulphur + 25 ppm nitrogen led towards similar conversions to that obtained in the absence of poisons over Al-MCM-41 (~ 80%) and Al-MTS (72%). However, n-HZSM-5 underwent a meaningful drop in conversion (20%), although the selectivity results are rather similar with those obtained without poisons.

The most remarkable results are attained when using the mixture of 1-hexene with concentrated poisons (7000 ppm sulphur + 250 ppm nitrogen). The conversion obtained over Al-MTS catalysts is similar to that achieved without poison whereas for Al-MCM-41, a slight decrease of around 7% is observed. However, the most striking data is shown over n-HZSM-5, wherein just a 27% conversion is obtained. This means a large drop in conversion highlighting that this catalyst is clearly affected by the long term operation in the presence of both poisons. According to the selectivity data obtained over Al-MTS, it seems that this catalyst is not affected at all by the presence of concentrated poisons. However, for the case of Al-MCM-41, an enhancement of dimers is appreciated. The results of conversion and selectivity over Al-MCM-41 are indicative of a slight deactivation. However, the most remarkable change in selectivity is observed over n-HZSM-5 zeolite. The selectivity towards dimers rises to 44.6% and especially, the selectivity towards hydrocarbons from cracking increases up to 23.2%. The oligomerization mechanism over this catalyst is thought to proceed by a combination of oligomerization-cracking

mechanism (path 3 and 5 of Figure 4) [44]. As a consequence of the large deactivation undergone by this catalyst, the oligomerization reaction is stopped at their very initial steps of the aforementioned mechanism.

Despite the hopeful results obtained over n-HZSM-5 in previous works [30,31], the strong external acid sites of this catalyst are finally deactivated by the concentrated poisons. These sites are indeed placed in/close to the micropore mouth and are responsible for the remarkable oligomerization performance of this catalyst (the standard micrometer HZSM-5 is quickly deactivated by pore blocking of its micropores [31]). We speculate about the strong adsorption of the poisons over these sites which neutralize them, rendering useless for oligomerization. According to this reasoning are the results of Chen et al. [22] that inactivate the external surface of HZSM-5 zeolite with 2,6 di-tert-butylpyridine. In addition, these poisons are known to be coke precursors [15,18] so the formation of coke/heavy oligomers over the external surface is also feasible. Al-MCM-41 and Al-MTS show pore sizes that allow the poison molecules free access without diffusional/steric hindrance to their acid sites which surprisingly does not bring about any heavy deactivation. In spite of the lower pore size of Al-MTS (1.8 nm) in comparison to Al-MCM-41 (2.3 nm), this is not detrimental to its performance. Several explanations might be brought to mind. Firstly, the high surface area of both catalysts ( $1000 \text{ m}^2 \text{ g}^{-1}$ ) could delay significantly the effect of the poisons on the deactivation of the acid sites. However, a more likely explanation ascribed their performance to their medium acid strength distribution as their sites show a lower trend towards bonding with the poisons. In this regard, the slight deactivation observed over Al-MCM-41 must be related to its slightly higher acid strength. Thus, Al-MTS presenting the weakest acid sites of the three tested catalysts as well as some extraframework aluminium (15-20%), which is known to generate Lewis acidity, shows the better performance not only because the

higher activity but also the slower deactivation by basic poisons, suggesting this catalyst as a rather judicious choice for testing the oligomerization of FCC effluents.

Simulated distillation analyses of the hydrocarbon mixtures resulting from the 1-hexene oligomerization reactions with the concentrated poisons (7000 ppm of sulphur + 250 ppm of nitrogen) were carried out in order to ascertain the presence of heavier compounds in the product mixture. It must be remarked that the “trusted” operational limit of the GC analysis used was around C<sub>25</sub> boiling point, since higher hydrocarbons are rather difficult to be properly determined. Consequently, simulated distillation analyses of the oligomerized samples were performed to estimate the real value of the fuel obtained following the operation method described in the Experimental Section. The simulated distillation analyses were performed on the previously distilled samples to remove the lighter products than n-nonane (unreacted hexenes and the solvent n-octane). Figure 4 illustrates the simulated distillation analyses (a) as well as their corresponding derivate curves (b). On the other hand, table 4 summarizes the temperatures corresponding to the 10%, 50%, 90% and 100% (T<sub>10%</sub>, T<sub>50%</sub>, T<sub>90%</sub> and T<sub>100%</sub> respectively) of distilled volume attained in the oligomerization products from the three tested catalysts. Al-MCM-41 and Al-MTS show similar simulated distillation analyses curves, although some subtle differences may be appreciated. Firstly, the Al-MTS simulated distillation curve is always below to that of Al-MCM-41, regardless of the chosen range. This means that lighter hydrocarbon products are achieved over Al-MTS than over Al-MCM-41 catalyst. Consequently, the respective T<sub>10%</sub>, T<sub>50%</sub>, T<sub>90%</sub> and T<sub>100%</sub> for Al-MTS are slightly lower than the values corresponding to Al-MCM-41 (see Table 4). Thereby, the respective temperature varies within the following ranges: T<sub>10%</sub> ~ 205-210, T<sub>50%</sub> ~ 295 – 305, T<sub>90%</sub> ~ 390 – 410 and T<sub>100%</sub> ~ 507 – 520°C. According to their respective boiling points, the higher temperatures correspond to the following n-paraffins: C<sub>12</sub> (T<sub>10%</sub>), C<sub>18</sub> (T<sub>50%</sub>), C<sub>26</sub> (T<sub>90%</sub>) and C<sub>40</sub> (T<sub>100%</sub>). By comparison with the data previously reported in the 1-

hexene oligomerization [31], the presence of poisons for both Al-MCM-41 and Al-MTS gives rise to a slight increase in distillation temperatures. On the other hand, the temperatures of the inflection points, determined by the derivative curve, are shown depicted in Figure 4b), similar over both Al-MCM-41 and Al-MTS catalysts.

The most remarkable results proceeds from n-HZSM-5. In accordance with the data of the GC analysis, only light hydrocarbons were produced after oligomerization of 1-hexene in the presence of concentrated poisons. Hence,  $T_{50\%}$ ,  $T_{90\%}$  and  $T_{100\%}$  drop to 158, 276 and 326°C, instead of the reported values without poisons of 299, 430 and 524°C, respectively [31]. This means that the highest molecular weight product obtained ( $T_{100\%}$ ) was near the boiling point of n-C<sub>19</sub> (~ 329°C) instead of the n-C<sub>40</sub> obtained in the absence of poisons ( $T_{\text{boiling point}} \sim 522^\circ\text{C}$ ). Hence, the presence of both concentrated poisons shortens distinctly the extent of the oligomerization paths over this catalyst. On the other hand, two inflection points were observed in the derivative curve, placed at 170 and 260°C which correspond roughly to n-decane ( $T_{\text{boiling point}} \sim 174^\circ\text{C}$ ) and n-tetradecane ( $T_{\text{boiling point}} \sim 252^\circ\text{C}$ ).

TG analyses of the three catalysts after the oligomerization experiments of 1-hexene + 7000 ppm sulphur + 250 ppm nitrogen mixture were performed in order to determine the nature and amounts of the adsorbed compounds. Figure 5 illustrates the obtained TG analyses. The total weight losses over the studied temperature range (50 – 600°C) were 12.7, 19.3 and 23.0% over n-HZSM-5, Al-MCM-41 and Al-MTS, respectively. These reported total weight losses over Al-MTS and Al-MCM-41 are meaningfully higher than those previously reported for the oligomerization of 1-hexene in absence of poisons [31]. Three different zones of weight loss may be envisaged within the graphs. Zone I encompasses the 50 – 171°C range, the latter temperature corresponding roughly to the n-C<sub>10</sub> paraffin boiling point (174°C). This zone is

ascribed to the removal of the light hydrocarbons adsorbed over the catalyst surface, mostly unreacted hexenes and the n-octane solvent. Additionally, the non-strongly bonded poisons are also desorbed in this zone, according to their respective boiling points ( $T_{bp}$  of 77 and 83°C for n-butylamine and thiophene, respectively). The weight losses obtained over both Al-MTS and Al-MCM-41 catalyst are fairly large in this range (around 8%), in contrast with the share obtained over n-HZSM-5 (0.9%). This surprisingly low value is indicative of neither the hexenes nor the solvent are really physically adsorbed on this catalyst, so the hexenes must undergo a quickly oligomerization over this catalyst or are removed during the TG pretreatment. The weight loss of zone II encompasses the temperature interval within 171 – 305°C, the latter corresponding roughly to n-C<sub>17</sub> paraffin ( $T_{bp} \sim 302^\circ\text{C}$ ). Zone II correspond to the removal of C<sub>10</sub> – C<sub>17</sub> hydrocarbons as well as to the combustion of non-strongly adsorbed oligomers. The weight losses in zone II vary within 4.4 – 7.2%. Both Al-MTS and Al-MCM-41 exhibit a continuous decline in zone II while for n-HZSM-5 a steep jump is appreciated. This could be indicative of the burn-off of the heavy oligomers non strongly adsorbed placed close to the pore mouth of the n-HZSM-5 micropores. This weight loss suggests the likely deactivation of the zeolite micropores by pore mouth blockage [45] or close to the external surface. Zone III comprises the weight loss within 305 – 600°C and corresponds to the removal of the strongly retained oligomers (coke) as well as to the dehydroxylation of the silanols placed at the catalyst surface. The weight losses are 4.6, 6.4 and 7.9% for n-HZSM-5, Al-MCM-41 and Al-MTS, respectively. By comparison with the reported data obtained in absence of poisons in the feed [31], which showed weight losses within 3.5 – 4.5%, a substantial increase is appreciated over Al-MTS and Al-MCM-41. Thus, higher coke yields are attained over both catalysts when the concentrated poisons are loaded in the feed, according to the promotional effect of such compounds in the generation of coke [17, 18].

The next step in this research was to test the performance of the Al-MTS catalyst in the oligomerization of a FCC effluent from a pilot plant setup provided by REPSOL-YPF. The experimental conditions used in this reaction were the standard ones:  $T = 200^{\circ}\text{C}$ ,  $P = 50 \text{ bar}$ ,  $\text{TOS} = 240 \text{ min.}$ , 30 wt.% naphta, 70 wt. % n-octane solvent and  $\text{WHSV} = 0.40 \text{ h}^{-1}$ . The makeup of the naphta effluent from FCC units is shown in table 5 and it is made up of a mixture of  $\text{C}_5 - \text{C}_{10}$  hydrocarbons. The major components were the  $\text{C}_6$  and  $\text{C}_7$  fractions (60 and 36%, respectively). The olefin content of the FCC effluent was of 70.6 wt.%. In this case, the conversion was based on both reacted hexenes and heptenes (their major components) and the selectivity was referred to in terms of boiling point fractions instead dimers, trimers, etc. because of the presence of heptenes in the feed. The results obtained in the oligomerization of the FCC effluent after a  $\text{TOS} = 240 \text{ min.}$  are illustrated in Figure 6. The measured conversion was of 58%, with a 33.6 % selectivity for the major product fraction  $\text{C}_{13} - \text{C}_{18}$ , followed by both  $\text{C}_9 - \text{C}_{12}$  and  $\text{C}_{19} - \text{C}_{30}$  in a close share (~ 26%). The selectivity towards  $\text{C}_3 - \text{C}_5$  hydrocarbons from cracking as well as to  $\text{C}_7 - \text{C}_8$  are around 5% and 9%, respectively, a bit higher than those achieved with the pure 1-hexene. However, it should be reminded that a certain amount of  $\text{C}_5 - \text{C}_{10}$  hydrocarbons are present initially in the feed, which may explain the higher share. Figure 7 exhibits the evolution of the measured conversion and selectivity towards the different fractions along the time on stream (TOS) up to 240 min. The conversion remains stable from 180 min. and the selectivity values from this point on also appears to vary just slightly, suggesting steady state operation after 180 min. of the oligomerization reaction. In addition, no indication of Al-MTS deactivation seems to be present at least in the range of the time on stream tested. In addition, the changes appreciated in the selectivity between 180 and 240 min. are just minor ones. The difference in conversion observed with regards to pure 1-hexene mixtures may be ascribed to the complex FCC effluent makeup. Not only other hydrocarbons from hexenes are present but also saturated hydrocarbons (paraffins, naphtenes, etc.), poisons, etc. Likewise, distilled simulation

analyses were performed according to the previously reported procedure in order to check the presence of heavy compounds hard to detect with our conventional GC analysis. Figure 8 illustrates the simulated distillation analysis of the hydrocarbon mixture obtained after distilling the product of the oligomerization of the FCC effluent after TOS = 240 min. As inferred from the graph, only  $T_{10\%}$  temperature ( $\sim 202^{\circ}\text{C}$ ) is similar to that attained in the oligomerization of the mixture of 1-hexene + 7000 ppm of sulphur + 250 ppm of nitrogen. The other three temperatures ( $T_{50\%}$ ,  $T_{90\%}$  and  $T_{100\%}$ ) obtained in the distillation of the FCC effluent are clearly higher, especially  $T_{90\%}$  and  $T_{100\%}$  ( $468$  and  $631^{\circ}\text{C}$ , respectively). This is likely caused by the presence of heptenes as well as up to  $\text{C}_{10}$  olefins in the effluent FCC feed which drives the oligomerization towards heavier compounds than with the pure 1-hexene feed. The derivative curve, shown at the bottom of Figure 8, exhibit four peaks placed at  $176$ ,  $251$ ,  $383$  and  $569^{\circ}\text{C}$ . However, the complex makeup of the FCC effluent feed makes these jumps not be as marked as they were observed with the pure 1-hexene feed. In summary and considering as a whole, these are really promising results regarding the potential future application of Al-MTS catalyst for the oligomerization of the olefins present in FCC naphthas.

#### 4. CONCLUSIONS

Several conclusions can be drawn from the reported data. Firstly, the activity and selectivity of both mesostructured catalysts remains practically unchanged (especially in Al-MTS case) under the presence of poisons, either alone or in combination, and even in concentrated amounts (250 ppm of nitrogen as n-butylamine + 7000 ppm sulphur as thiophene). This rather remarkable performance has been ascribed to its high surface area and to its medium acid strength distribution that disallows strong bonding with the poisons at the working temperature. Additionally, TG analyses point out a 6-8% of weight loss within  $400 - 500^{\circ}\text{C}$  over the Al-MTS

and Al-MCM-41 catalysts, suggesting the deposition of certain amount of coke. According to simulated distillation analysis, the distilled product after oligomerization of the 1-hexene + 250 ppm of nitrogen (as n-butylamine) + 7000 ppm of sulphur (as thiophene) over Al-MTS and Al-MCM-41 is just slightly heavier than those attained with the pure 1-hexene feed, remarking the promotional effect of such compounds in the generation of coke in this process.

Nanocrystalline n-HZSM-5 catalyst performance was strongly affected by the presence of the concentrated poison feed, decreasing abruptly its conversion. Additionally, the selectivity was addressed towards lighter hydrocarbons, as no oligomers heavier than C<sub>19</sub> were measured (instead of the C<sub>36</sub> - C<sub>40</sub> over the two mesostructured catalysts), suggesting an effective shortening in the oligomerization paths. This was indicative of a deactivation by strong adsorption of the poisons over both the external surface and inside the micropores, as well as of coke/heavy oligomers deposition, which causes micropore blockage.

Al-MTS also exhibited remarkable performance in the oligomerization of the FCC effluent giving rise to a reasonable conversion with a 33% selectivity towards C<sub>13</sub> – C<sub>18</sub> in the reaction conditions used. Seemingly, the catalyst did not undergo deactivation after a TOS = 240 min, the differences with regards to pure 1-hexene feed being ascribed to their complex makeup of mostly hexenes (60.0%) and heptenes (36.0%) with 70.6% olefin content. Heavier oligomer products were measured in the simulated distillation analyses, mainly due to the presence of heptenes and even up to C<sub>10</sub> olefins in the feed.

## 5. ACKNOWLEDGMENTS

The authors want to thank *Ministerio de Ciencia y Tecnología* (Project CICYT CTQ2005-09078/PPQ) for the financial support to this research. We are also grateful to REPSOL-YPF for providing the FCC naphta sample used in this research.

## 6. REFERENCES

- [1] G. Ertl, H. Knozinger, J. Weitkamp, Handbook of Heterogeneous Catalysis, Wiley-VCH, Weinheim, 1997.
- [2] V. N. Ipatieff, B. B. Corson, G. Egloff, Ind. Eng. Chem. 27 (1935) 1077 - 1081.
- [3] R. J. Quann, L. A. Green, S. A. Tabak, F. J. Krambeck, Ind. Eng. Chem. Res. 27 (1988) 565 - 570.
- [4] G. F. Froment, J. De Meyer, E. G. Derouane, J. Catal. 124 (1990) 391 - 400.
- [5] E. Piera, C. Téllez, J. Coronas, M. Menéndez, J. Santamaría, Catal. Today, 67 (2001) 127 - 138.
- [6] S. A. Tabak, F. J. Krambeck, W. E. Garwood, AIChE J. 32 (1986) 1526 - 1531.
- [7] H. van Bekkum, E. M. Flanigen, Introduction to Zeolite Science and Practice, Elsevier: Amsterdam, 2001.

- [8] S. Matar, L. F. Hatch, Chemistry of Petrochemical Processes, Gulf Professional Publishing, Butterworth-Heinemann (2001).
- [9] G. Bellusi, P Pollesel, Stud. Surf. Sci. Catal. 158 (2005) 1201 – 1211.
- [10] G. A. Olah, A. Molnar, Hydrocarbon Chemistry, John Wiley & Sons, New York, 1995.
- [11] D. A. Lomas, US Patent 20040140246 A1 (2004).
- [12] C. Marcilly, Stud. Surf. Sci. Catal. 135 (2001) 37.
- [13] C. Marcilly, J. Catal. 216 (2003) 47 - 62.
- [14] X. Dupain, M. Makkee, J. A. Moulijn, Appl. Catal. A-Gen. 297(2) (2006) 198 - 219.
- [15] S. Ng, Y. Zhu, A. Humphries, L. Zheng, F. Ding, L. Yang, S. Yui, Energy Fuels 16 (2002) 1209 - 1221.
- [16] J. B. Green, E. J. Zagula, L. L. Young, Symp. Petrol. Chem. Process. (1995) 691 - 694.
- [17] A. Corma, C. Martinez, G. Ketley, G. Blair, Appl. Catal. A-Gen. 208 (2001) 135 - 152.
- [18] L. B. Galperin, Appl. Catal., A-Gen. 209 (2001) 257 - 268.

[19] J. M. Dakka, H. K. T. Goris, G. M. K. Mathys, S. H. Brown, B. R. Cook, Exxon Mobil Chemical Company, US Patent 20040220440 (2004).

[20] W. E. Garwood, ACS Symp. Ser. 218 (1983) 383 - 396.

[21] N. S. Gnep, F. Bouchet, M. R. Guisnet, Prepr. – Am. Chem. Soc. Div. Pet. Chem. 36(4) (1991) 620 - 626.

[22] C. S. H. Chen, R. F. Bridger, J. Catal. 161 (1996) 687 - 693.

[23] J. E. Stanat, G. M. K. Mathys, D. W. Turner, WO Patent 2003082780 A1 (2003).

[24] A. Giusti, S. Gusi, G. Bellussi, V. Fattore, Eur. Pat. Appl. EP Patent 290068 A1 (1988).

[25] J. A. Martens, R. Ravishankar, I. E. Mishin, P. A. Jacobs, Angew. Chem. Int. Ed. 39(23) (2000) 4376 - 4379.

[26] H. Abrevaya, R. Frame, US Patent 6403853 B1 (2002).

[27] S. Peratello, C. Perego, G. Bellusi, US Patent 5,342,814 (1994).

[28] B. Chiche, E. Sauvage, F. Di Renzo, I. I. Ivanova, F. Fajula, J. Mol. Catal. A: Chem. 134 (1998) 145 - 157.

[29] V. Hulea, F. Fajula, J. Catal. 225 (2004) 213 - 222.

- [30] R. Catani, M. Mandreoli, S. Rossini, S., A. Vaccari, *Catal. Today* 75 (2002) 125 - 131.
- [31] R. Van Grieken, J. M. Escola, J. Moreno, R. Rodriguez, *Appl. Catal. A-Gen.* 305 (2006) 176 - 188.
- [32] J. M. Escola, R. Van Grieken, J. Moreno, R. Rodriguez, *Ind. Eng. Chem. Res.* 45 (2006) 7409 - 7414.
- [33] J. P. G. Pater, P. A. Jacobs, J. A. Martens, *J. Catal.* 184 (1) (1999) 262 - 267.
- [34] M. Yamamura, K. Chaki, T. Wakatsuki, H. Okado, K. Fujimoto, *Zeolites* 14 (8) (1994) 643 - 649 .
- [35] R. Van Grieken, J. M. Escola, R. Rodríguez, *Stud. Surf. Sci. Catal.* 158 (2005) 1733 - 1740.
- [36] A. de Klerk, *Ind. Eng. Chem. Res.* 44 (2005) 3887 - 3893.
- [37] J. P. G. Pater, P. A. Jacobs, J. A. Martens, *J. Catal.* 179 (1998) 477 - 482.
- [38] R. Van Grieken, J. L. Sotelo, J. M. Menéndez, J. A. Melero, *Microporous Mesoporous Mater.* 39(1-2) (2000) 135 - 147.
- [39] W. Lin, Q. Cai, W. Pang, Y. Yue, B. Zou. *Microporous Mesoporous Mater.* 33 (1999) 187 - 196.

- [40] J. Aguado, D. P. Serrano, J. M. Escola, *Microporous Mesoporous Mater.* 34 (2000) 43 - 54.
- [41] J. Aguado, D. P. Serrano, G. San Miguel, J. M. Escola, J. M. Rodriguez, *J. Anal. Appl. Pyrolysis* 78(1) (2007) 153 - 161.
- [42] R. Van Grieken, D. P. Serrano, J. A. Melero, A. Garcia, *J. Mol. Catal. A: Chem.* 222(1-2) (2004) 167 - 174.
- [43] J. Aguado, D. P. Serrano, J. M. Escola, J. M. Rodriguez, *Microporous Mesoporous Mater.* 75(1-2) (2004) 41 - 49.
- [44] O. Klepel, A. Loubentsov, W. Böhlmann, H. Papp, *Appl. Catal. A-Gen.* 255(2) (2003) 349 - 354.
- [45] K. G. Wilshier, P. Smart, R. Western, T. Mole, T. Behrsing, *Appl. Catal.* 31(2) (1987) 339 - 354.

## FIGURE CAPTIONS

**Figure 1.** XRD patterns of the calcined a) n-HZSM-5, b) Al-MCM-41 and Al-MTS catalysts.

**Figure 2.** Simplified network of the 1-hexene oligomerization reactions.

**Figure 3.** Conversions and selectivities obtained in the oligomerization of the 1-hexene + thiophene + n-butylamine-constituting feedstocks over the three catalysts (T = 200°C, P = 50 bar, TOS = 240 min, WHSV= 0.40 h<sup>-1</sup>, 30 % 1-hexene).

**Figure 4.** Simulated distillation (a) and derivative curves (b) of the hydrocarbon mixtures obtained after distilling the products from the oligomerization of 1-hexene + 7000 ppm sulphur (as thiophene) + 250 ppm nitrogen (as n-butylamine) over the three catalysts (T = 200°C; WHSV = 0.40 h<sup>-1</sup>; P = 5 MPa; TOS = 240 min.; solvent = n-octane).

**Figure 5.** TG analyses of the three catalysts after reaction with the 1-hexene + 7000 ppm sulphur (as thiophene) + 250 ppm nitrogen (as n-butylamine) mixture.

**Figure 6.** Conversion and selectivities obtained in the oligomerization of a FCC naphta effluent over Al-MTS (T = 200°C, P = 50 bar, TOS = 240 min, WHSV= 0.40 h<sup>-1</sup>, 30 wt. % FCC effluent).

**Figure 7.** Evolution with time on stream (TOS) of the conversion and selectivities attained in the oligomerization of the FCC effluent (T = 200°C, P = 50 bar, WHSV = 0.40 h<sup>-1</sup>, 30 wt. % FCC effluent).

**Figure 8.** Simulated distillation analysis curve of the hydrocarbon mixture obtained after distilling the products from the oligomerization of the FCC effluent over the Al-MTS catalyst (T = 200°C, WHSV = 0.40 h<sup>-1</sup>, P = 50 bar, TOS = 240 min., 30 wt.% FCC effluent).

**Table 1.** Physicochemical properties of the calcined catalysts.

Properties	n-HZSM-5	Al-MCM-41	Al-MTS
Si/Al <sup>a</sup>	32	31	32
A <sub>BET</sub> (m <sup>2</sup> g <sup>-1</sup> )	395	1200	1290
V <sub>pore</sub> (cm <sup>3</sup> g <sup>-1</sup> ) <sup>b</sup>	0.16	0.85	0.86
D <sub>pore</sub> (nm) <sup>c</sup>	0.55 (*)	2.30	1.80
Acidity (meq NH <sub>3</sub> g <sup>-1</sup> ) <sup>d</sup>	0.32	0.15	0.14
T <sub>max</sub> (°C) <sup>e</sup>	355	265	260

<sup>a</sup> Determined by ICP analysis. <sup>b</sup> Measured at P/P<sub>0</sub> = 0.95.

<sup>c</sup> Determined from the maximum of the BJH pore size distribution except sample (\*).

<sup>d</sup> Calculated from ammonia TPD measurements

<sup>e</sup> Temperature for maximum ammonia desorption

**Table 2.** Conversions and selectivities obtained in the oligomerization of 1 hexene + 700 ppm sulphur (as thiophene) over the three catalysts

<b>Catalysts</b>	<b>Thiophene</b>	<b>X<sub>hexenes</sub></b>	<b>S<sub>cracking</sub></b>	<b>S<sub>dimers</sub></b>	<b>S<sub>trimers</sub></b>	<b>S<sub>heavy</sub></b>	<b>S<sub>others</sub></b>
Al-MTS	No	75.8	2.9	30.2	31.5	33.3	2.1
Al-MTS	Yes	79.0	2.6	32.2	30.1	33.1	2.0
Al-MCM-41	No	78.6	2.0	37.6	31.9	26.9	1.6
Al-MCM-41	Yes	82.0	5.0	31.6	30.2	31.5	1.7
n-HZSM-5	No	90.0	1.1	38.3	33.7	24.3	2.6
n-HZSM-5	Yes	79.1	1.4	41.4	31.2	23.6	2.4

Conditions: T = 200°C, P = 50 bar, TOS = 240 min, WHSV= 0.40 h<sup>-1</sup>, 30 % 1-hexene.

**Table 3.** Conversions and selectivities obtained in the oligomerization of 1 hexene + 25 ppm of nitrogen (as n-butylamine) over the three catalysts

<b>Catalysts</b>	<b>n-butylamine</b>	<b>X<sub>hexenes</sub></b>	<b>S<sub>cracking</sub></b>	<b>S<sub>dimers</sub></b>	<b>S<sub>trimers</sub></b>	<b>S<sub>heavy</sub></b>	<b>S<sub>others</sub></b>
Al-MTS	No	75.8	2.9	30.2	31.5	33.3	2.1
Al-MTS	Yes	71.0	5.1	32.7	26.3	32.2	3.7
Al-MCM-41	No	78.6	2.0	37.6	31.9	26.9	1.6
Al-MCM-41	Yes	80.5	3.3	34.0	33.2	27.0	2.5
n-HZSM-5	No	90.0	1.1	38.3	33.7	24.3	2.6
n-HZSM-5	Yes	75.0	2.7	39.2	31.1	24.6	2.4

Conditions: T = 200°C, P = 50 bar, TOS = 240 min, WHSV= 0.40 h<sup>-1</sup>, 30 % 1-hexene.

**Table 4.** Temperatures corresponding to 10% ( $T_{10\%}$ ), 50% ( $T_{50\%}$ ), 90% ( $T_{90\%}$ ) and 100% ( $T_{100\%}$ ) of the collected volumes in the simulated distillation analyses.

<b>Catalysts</b>	<b>Temperatures (°C)</b>			
	<b><math>T_{10\%}</math></b>	<b><math>T_{50\%}</math></b>	<b><math>T_{90\%}</math></b>	<b><math>T_{100\%}</math></b>
Al-MTS	205	297	391	507
Al-MCM-41	209	306	412	519
n-HZSM-5	138	158	276	326

**Table 5.** Composition of the FCC effluent.

<b>Carbon number</b>	<b>Composition<sup>a</sup> (%)</b>
5	2.0
6	60.0
7	36.0
8	0.9
9	0.5
10	0.6

<sup>a</sup>Calculated from GC analysis.

FIGURE 1 a)

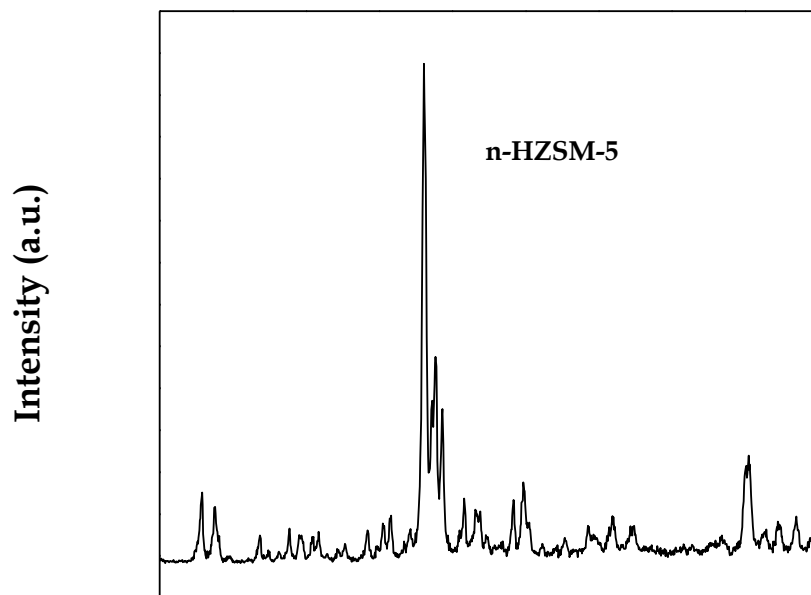


FIGURE 1 b)

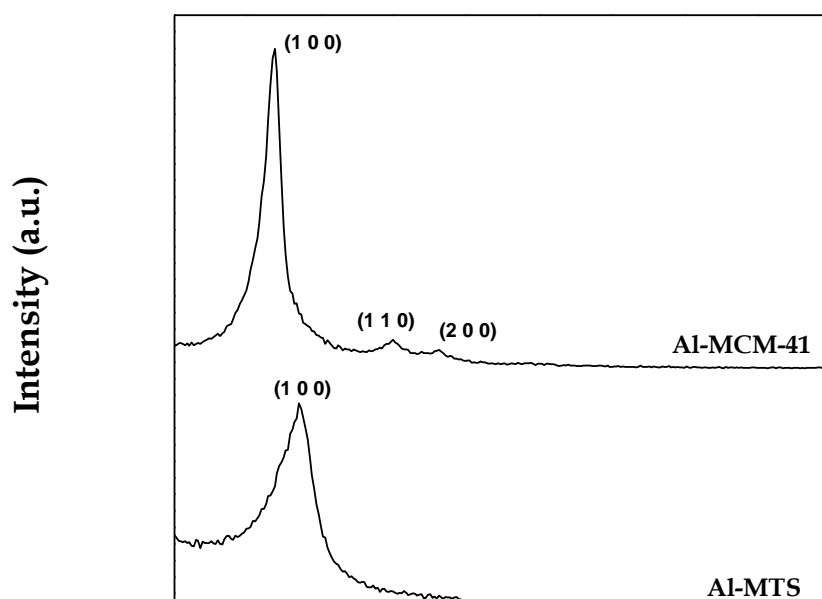


FIGURE 2

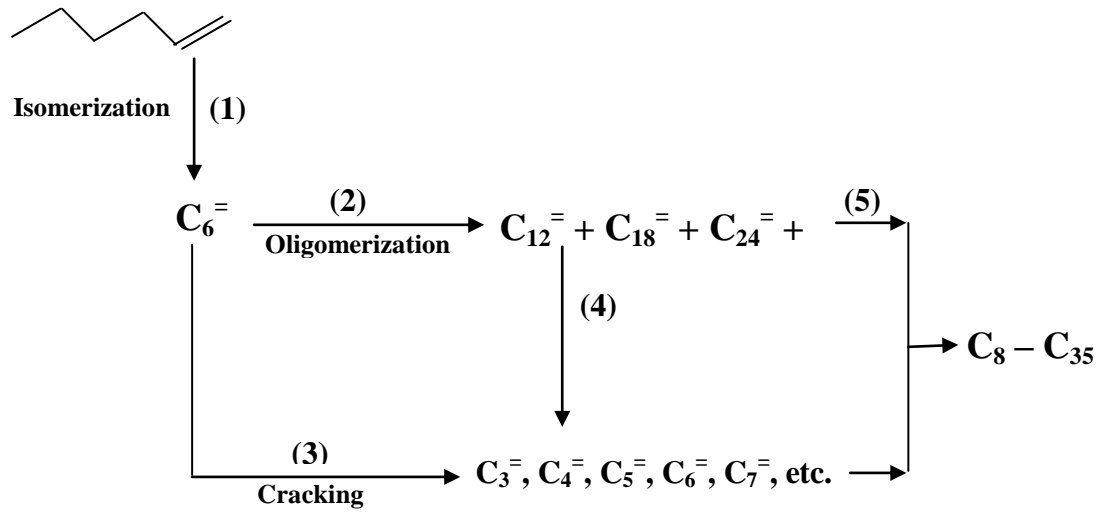


FIGURE 3

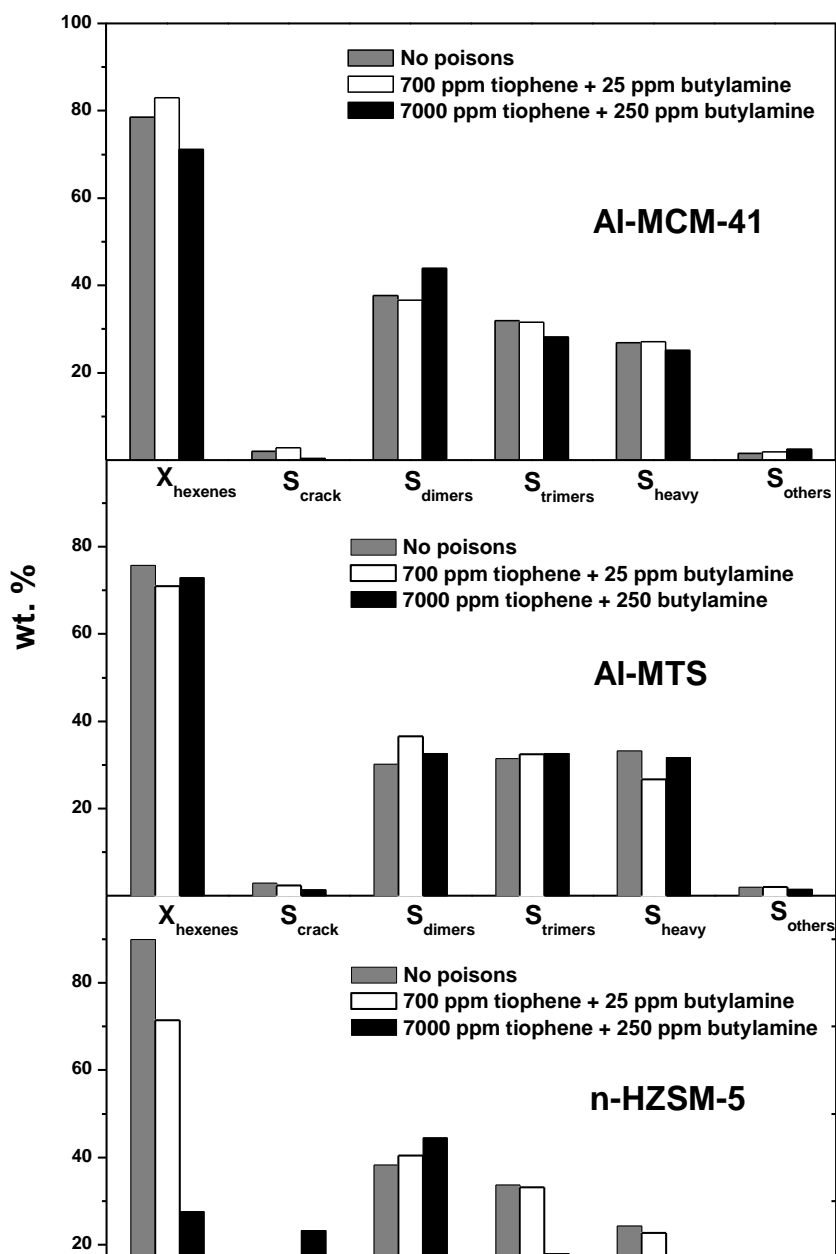


FIGURE 4

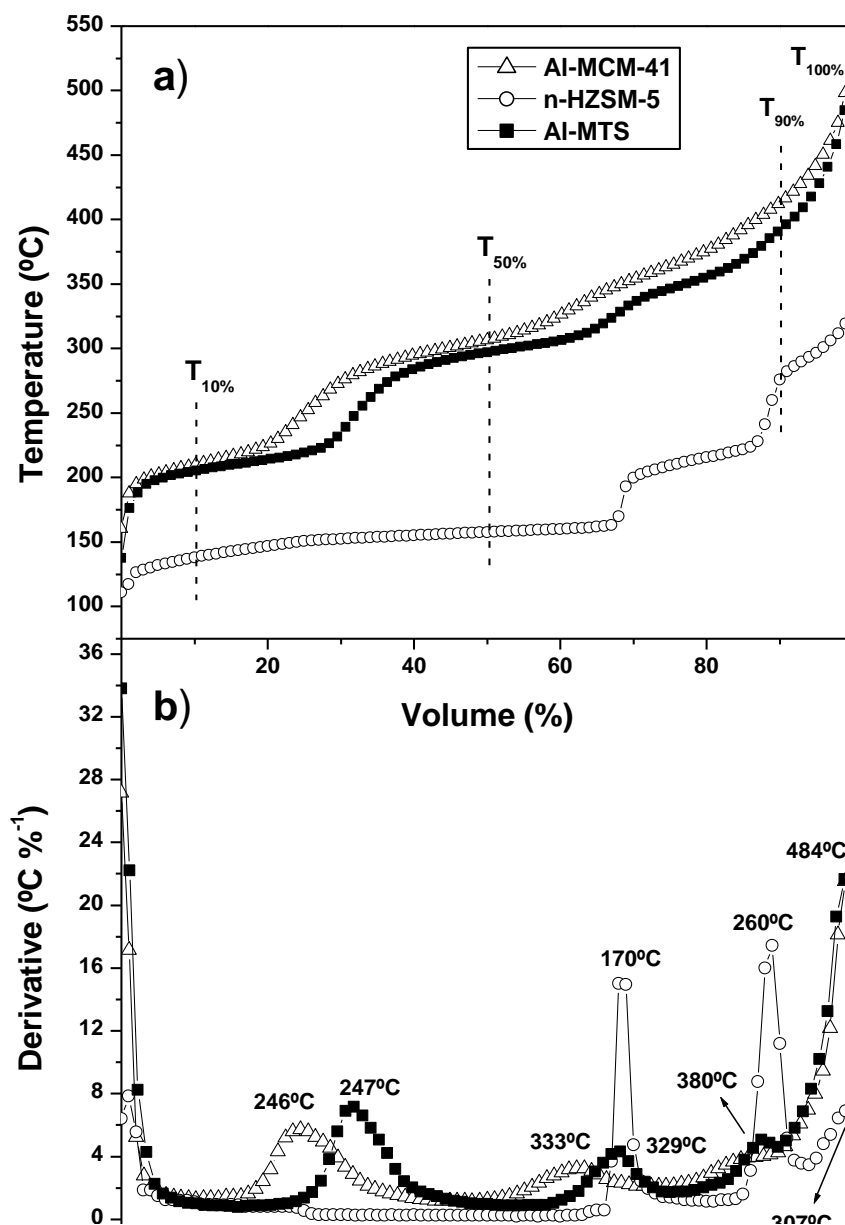


FIGURE 5

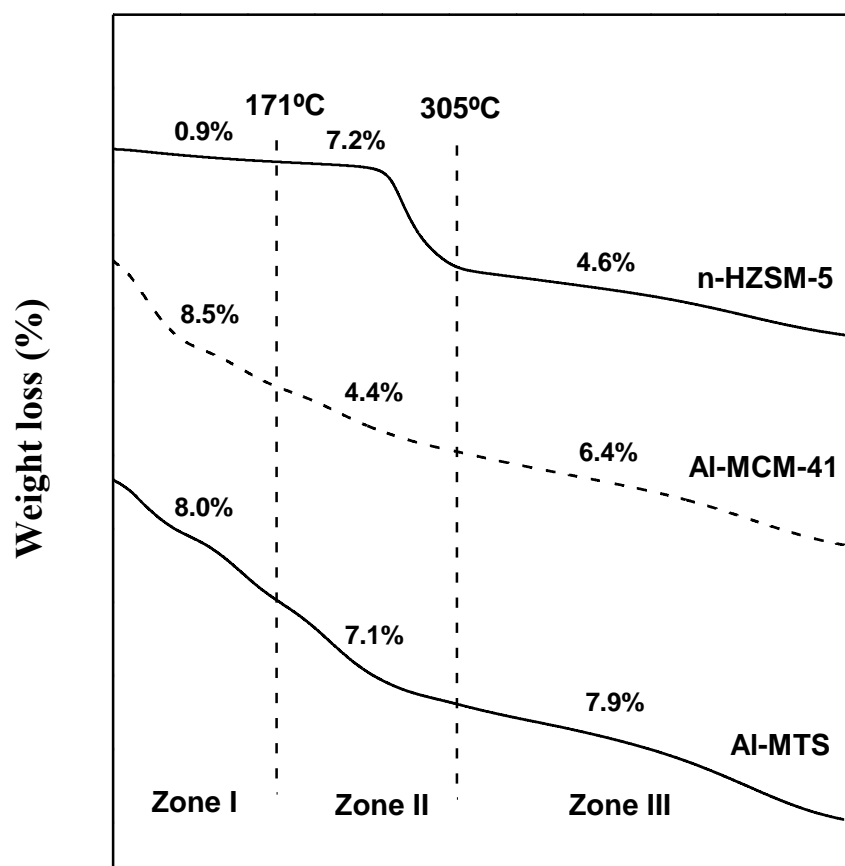


FIGURE 6

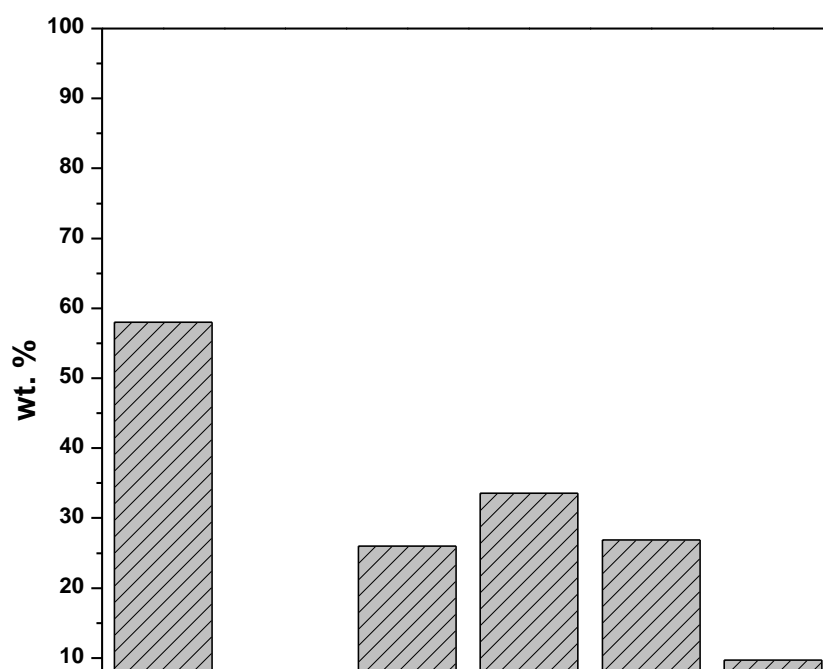


FIGURE 7

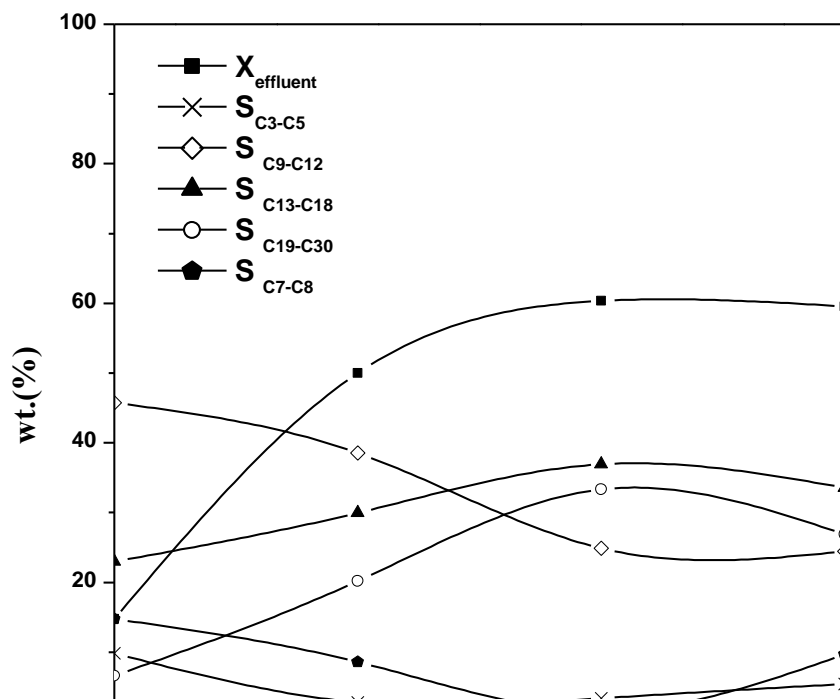


FIGURE 8

